Concepts for the MEIC Interaction Point Beam Pipe

Charles E. Hyde*
Old Dominion University, Norfolk VA 23529

(Dated: 22 July 2015)

version 2.2

CONTENTS

* chyde@odu.edu

I. INTRODUCTION

Designing the beam pipe through the Interaction Point (IP) of MEIC design requires optimizing multiple, sometimes contradictory, requirements. A few key issues include:

- Mechanical stability under vacuum;
- Maintain high vacuum and adequate Beam Stay Clear (BSC) for the primary beams (including during injection/acceleration);
- High RF conductance and good impedance matching for beam-induced RF fields;
- Thin walls and/or exit windows for all detectable scattered particles;

These notes are primarily focussed on the downstream ion beam line.

The coordinate system and drawings in this note assume that ion beam momentum direction at the IP is

$$\hat{P} = \hat{z}\cos(0.050) + \hat{x}\sin(0.050) \tag{1}$$

In reality, the current design has $\hat{P}\cdot\hat{x} < 0$ at each IP. Thus all drawings can be considered as "views from the bottom".

A. Beam Emittance and Beam Stay Clear

The beam emittance and β^* values at the full acceptance IP are summarized in Table I. The rms size and rms angular spread of the beams at the IP are:

$$\sigma(x,y) = \sqrt{(\epsilon_{N;x,y}/\gamma)\,\beta^*_{x,y}} \qquad \text{and} \quad \sigma(x',y') = \sqrt{\epsilon_{N;x,y}\,/\,\left(\gamma\beta^*_{x,y}\right)} \tag{2}$$

(where γ is the relativistic boost, not the Courant-Snyder parameter). The Beam Stay Clear (BSC) is calculated at $10\sigma(x,y)$.

As a consequence of the electron-cooling of the ion beams in both the Booster and the main ring, the ion beam normalized emittances are expected to be independent of momentum, and for steady state collisions at any ion rigidity $P/Z \in [20, 100]$ GeV/c. The β^* values are assumed independent of ion rigidity, and therefore both the rms beam size and rms angular spread at the IP grow as $1/\sqrt{P/Z}$. This is reflected in Table I in the entries for the BSC at the entrance to the downstream FF Q1 for ion beam rigidities $P/Z = 20$ GeV/c. During acceleration, the beam envelope will be increased at the IP and decreased in the quads. However, the BSC values for Pb indicate that there must be a large vacuum pipe through the FFQ if we wish to preserve the option of low-energy high-luminosity running on heavy ions. This could be important, for example, for measuring the Q^2-evolution of the EMC effect, and extracting the gluon EMC effect. Note, however, that if the minimum momentum for Pb is raised to $Z \cdot 21$ GeV/c, then the BSC at the entrance to FFQ1 is 7.7 cm.

TABLE I.
MEIC Design parameters *circa* April 2015 [1]. The electron rms bunch length is 1.2 cm. All ion beam bunch lengths are 1.0 cm. The ion beam currents are 0.5 Amp, independent of Z, consequently the number of particles per bunch scales as $1/Z$. For $e-Pb$ collisions the β-functions of the electron beam are relaxed to $\beta^*_{x,y} = 4,\ 2$ cm to match the Pb beam rms size at the IP. Luminosity is per nucleon.

	Beam →	Electron	Proton	Deuteron	Helium	Carbon	Calcium	Lead
Parameter	Units	e^-	p	d	$^3He^{++}$	$^{12}C^{6+}$	$^{40}Ca^{20+}$	$^{208}Pb^{82+}$
Momentum	GeV/c	5	100	100	200	600	2000	8200
Normalized Emittance								
Horizontal	10^{-6} m rad	144	1	0.5	0.7	0.5	0.5	0.5
Vertical	10^{-6} m rad	72	0.5	0.25	0.35	0.25	0.25	0.25
Parameters at the Full Acceptance IP								
$\beta^*_{\rm Horiz}/\beta^*_{\rm Vert}$	cm	2.6/1.3	4/2	4/2	4/2	4/2	4/2	5/2.5
$\sigma(x)/\sigma(y)$	μm	19/9.7	19/9.7	19/9.7	20/9.9	19/9.6	19/9.6	22/11
$\sigma(x') = \sigma(y')$	mrad	0.744	0.484	0.484	0.495	0.482	0.482	0.543
Luminosity	$(\text{nb}\cdot\text{sec})^{-1}$		4.6	9.2	6.6	9.2	9.2	7.8
Beam Stay Clear at $s = 7$ m (Entrance to FF Q1). Units of P/Z are GeV/c.								
BSC ($P/Z = 100$)	cm	—	±3.4	±3.4	±3.5	±3.4	±3.4	±3.8
BSC ($P/Z = 20$)	cm	—	±7.6	±7.6	±7.7	±7.5	±7.5	±8.5

B. Final Focus Quadrupole-Triplet Acceptance

TABLE II. **Ion Downstream Dipole-1 and FFQ Triplet**
The coordinate $z(Qi)$ is the distance from the IP to the magnetic center of each magnet, of magnetic length $L(Qi)$. If it is possible to build higher field magnets, the gradients will remain the same, but the apertures will increase proportionally [2].

Parameter	Units	$D1$	$Q1$	$Q2$	$Q3$
$\partial B_x/\partial y$	T/m	0	89	−51	36
B(Max)	T	2	8	8	6.3
R(inner)	cm	15	9	16	17.5
R(outer)	cm	–	16	23	25
$z(Qi)$	m	5.5	7.6	10.4	13.2
$L(Qi)$	m	1.0	1.2	2.4	1.2

The design specifications of the three downstream ion Final Focus Quads (FFQ) are listed in Table II. The FFQ apertures create a line of sight acceptance for neutrons (and gamma's) from the target as follows:

$$\approx \text{Circular cone, opening angle } \theta = \pm 12 \text{ mrad, centered at } \quad (x'_0, y'_0) = (2, -3) \text{ mrad.} \quad (3)$$

The positive x-direction is in the horizontal plane directed away from the electron beam line and the positive y-direction is vertically up [2]. The vertical displacement of the neutral acceptance is a consequence of the solenoidal field. For charged particles, the acceptance of the full FFQ optics is momentum dependent. For magnetic rigidity of the scattered (or spectator) particle $P'/Z' \in [100\%, 150\%]P/Z$ (where P/Z is the rigidity of the incident

beam) the acceptance is approximately elliptical, with semi-major axes:

$$\pm\,10 \text{ mrad horizontal,} \qquad \text{and} \quad \pm\,12.5 \text{ mrad vertical,} \tag{4}$$

projected back to the IP, and relative to the incident ion direction. As the momentum of the scattered particle decreases, the $x' > 0$ acceptance is reduced, reaching about +7 mrad at $P'/Z' = 50\%P/Z$ (*e.g.* spectator protons in the deuteron).

II. BEAM PIPE MATERIALS, MECHANICAL REQUIREMENTS, AND RADIATION LENGTH

TABLE III. Young's Modulus E, Radiation Length X_0, Figure of Merit $X_0\sqrt[3]{E}$, and minimum wall thickness to radius ratio t/R for a circular vacuum pipe, for common materials used in accelerator beam pipes.

Material →		Be	CFC*	Al-Be	Al	Ti	Fe**	Air	RF mesh†
Parameter	Units								
E	GPa	290	200	193	70	110	210	—	
X_0	cm	35.3	27.1	25.3	8.9	3.6	1.8	$3.0 \cdot 10^4$	46.3
$X_0\,E^{1/3}$		2.34	1.58	1.46	0.37	0.17	0.11	—	
t/R	%	2.15	2.43	2.46	3.45	2.97	2.39	—	

* Carbon Fibre Composite

** Stainless Steel

†RADIOSCREEN$^{\text{TM}}$, `www.lessEMF.com`: $X_0 = 23.13$ cm, Thickness 0.09 mm,
Areal density 0.0045 g/cm^2
By weight: 23.4% Cu; 10.9% Ni; 65.7% Polyester thread

A. Mechanical Requirements of the Beam Line Vacuum Pipe

The ion beam pipe is likely to be either circular, or conical with a small angular opening (of order of the 12 mrad acceptance of the FFQ optics). For a long cylindrical vacuum pipe, the required wall thickness t as a function of radius R (including $\times 2$ safety margin) is ([3], Eq. 4):

$$\frac{t}{R} = 2\left[\frac{P_{\text{atm}}(1-v^2)}{0.25E}\right]^{1/3}, \tag{5}$$

where E is Young's Modulus of the material and v is Poisson's ratio of the transverse contraction strain to longitudinal stretch strain. The value of $1 - v^2$ is generally close to 0.9 [3]. Values of E and t/R for common materials are listed in Table III. Over a broad range of materials, the required thickness to radius ratio is 2 to 3 %, including safety margin.

B. Multiple Scattering Figure of Merit

For a charged particle of momentum P, energy E, and charge ze exiting the vacuum at an angle α to the local plane of the pipe (of perpendicular thickness t), the rms multiple scattering angle is ([4], Chapter 32§3):

$$\theta_{m.s.} = z\frac{13.5 \text{ MeV/c}}{p}\sqrt{\frac{t}{X_0 \sin\alpha}}\left[1 + 0.038 \ln \frac{z^2 t}{X_0 \sin\alpha}\right] \tag{6}$$

where X_0 is the radiation length of the material. For different materials, the required thickness t scales as $E^{-1/3}$, as defined in Eq. 5. Neglecting the log term in the multiple scattering, the figure of merit (Table III) scales as:

$$\text{F.O.M.} \propto X_0 E^{1/3}. \tag{7}$$

Table III illustrates the Be is the best material, almost a factor of two better than its nearest competitors, Carbon-Fibre-Composite (CFC) or Be-Al alloys. Use of a CFC beam pipe would require an inner coating of Al, or other conductive material. The RF skin depth of a conductor of magnetic permeability μ and resistivity ρ is (SI units):

$$\lambda = \sqrt{\frac{\rho}{\pi f \mu}}. \tag{8}$$

The skin depth of Al at 100 MHz is $\sim 10\,\mu$m and at 1 GHz it is $< 3\,\mu$m. The light weight mesh listed in Table III has an RF attenuation rating of 50 dB from 20 MHz to 3 GHz.

C. Consequences for Beam Pipe Design

If a 14 GeV/c singly charged particle exits the vacuum at normal incidence through a 1 cm thick Al window, the rms multiple scattering is 0.3 mrad, with is less than the intrinsic beam spread at the IP. If this exit is 1 m from the IP, the projected vertex resolution is 0.3 mm – still excellent. On the other hand, if the same particle exits through a 1 mm thick Al pipe at an incidence of 14 mrad, the multiple scattering angle is 0.9 mrad: Perhaps not catastrophic, but significantly worse. The worst case is if a particle at 15 mrad exits through a conical beam pipe flaring at 14 mrad. Then the angle of incidence is only 1 mrad, the exit point is much further downstream and the multiple scattering angle is ~ 4 mrad.

The likely optimal solution for the beam pipe is a cone, with a series of steps to allow particles to exit at approximately normal incidence. This will likely create small regions of phase space with almost infinite material thickness. This is probably better than having large regions of phase space with finite but thick windows.

III. FORWARD DETECTION

On the downstream ion side, the detector can be divided into four regions: Central (or Barrel), Endcap, Forward, and Far-Forward. The Far-Forward region consists of all

tracking detectors located after the FFQ triplet. This can be further separated into detectors upstream and downstream of the large 60 mrad bend dipole. The acceptance of the Far-Forward region was described in §I B. The Forward region is defined by all particles that pass through the dipole D1 in front of Q1, but are outside the FFQ acceptance.

The D1 magnet is not designed yet, so its acceptance is not fully determined. However, its basic property is a 1 m magnetic length with total $\int \mathbf{B} \times d\mathbf{l} = 2$ Tesla meter at $P_0 = 100$ GeV/c. This gives a 6 mrad bend angle. There are three basic concepts for D1:

- A single septum style magnet, parallel to electron beam line, with the maximal acceptance compatible with zero field integral on the electron beam line.
- A pair of opposite field dipoles, on either side of the electron beam line. The symmetry guarantees zero field on the electron beam line, but there is still a large quadrupole field that needs to be cancelled by a superconducting tube, or a hybrid cloaking device of an outer Fe shell and an inner superconductor. This dipole pair would provide improved analysis of scattered particles emitted at > 60 mrad from the ion beam, on the incoming electron beam side.
- A single large dipole straddling the electron beam line. This optimizes the detection acceptance, but the electron beam line shielding is much more difficult.

A preliminary design of the first option has an angular acceptance (at the entrance) of close to 30 mrad [5]. However, for design purposes we assume a dipole whose large angle side extends to 100 mrad relative to the electron beam line. Consequently, for either of the latter two designs, we can assume that the 'Forward' region occupies the geometrical space of ± 100 mrad relative to the solenoid axis (electron beam line).

The primary purpose of the Dipole and detectors behind it, is to analyze the 'target fragmentation' region of DIS events. This should be dominated by pions with small transverse momenta (of order 200 MeV/c) and longitudinal momenta up to $(ZP_0/A)(m_\pi/M_N)$. For 100 GeV incident protons, this is $p_\pi \leq 14$ GeV/c. These pions will have a deflection in D1 of $\theta_\pi \geq 42$ mrad. For example, for a diffractively produced Δ with a forward momentum of 100 GeV/c, the rms $|\mathbf{p}_\perp|$ of the decay pion is 186 MeV/c and the rms emission angle of the pion relative to the ion beam is 12 mrad. At the opposite end of the kinematic phase space, if the baryonic remnant has very high mass (approaching $W^2 = (q + P)^2$), the spectrum of forward mesons extends almost up to the incident beam momentum.

IV. BEAM PIPE DESIGN

What follows are preliminary ideas. A full design of the beam pipe will require optimization of particle tracking resolution, mechanical tolerances, and physics prioritization. This must be an iterative process, with resolution and acceptance students based on a preliminary design.

The basic philosophy of the present design is to provide minimal multiple scattering ($X/X_0 < 0.1$ including exit angle) over the full acceptance region. This requires several narrow angular regions of almost infinite thickness.

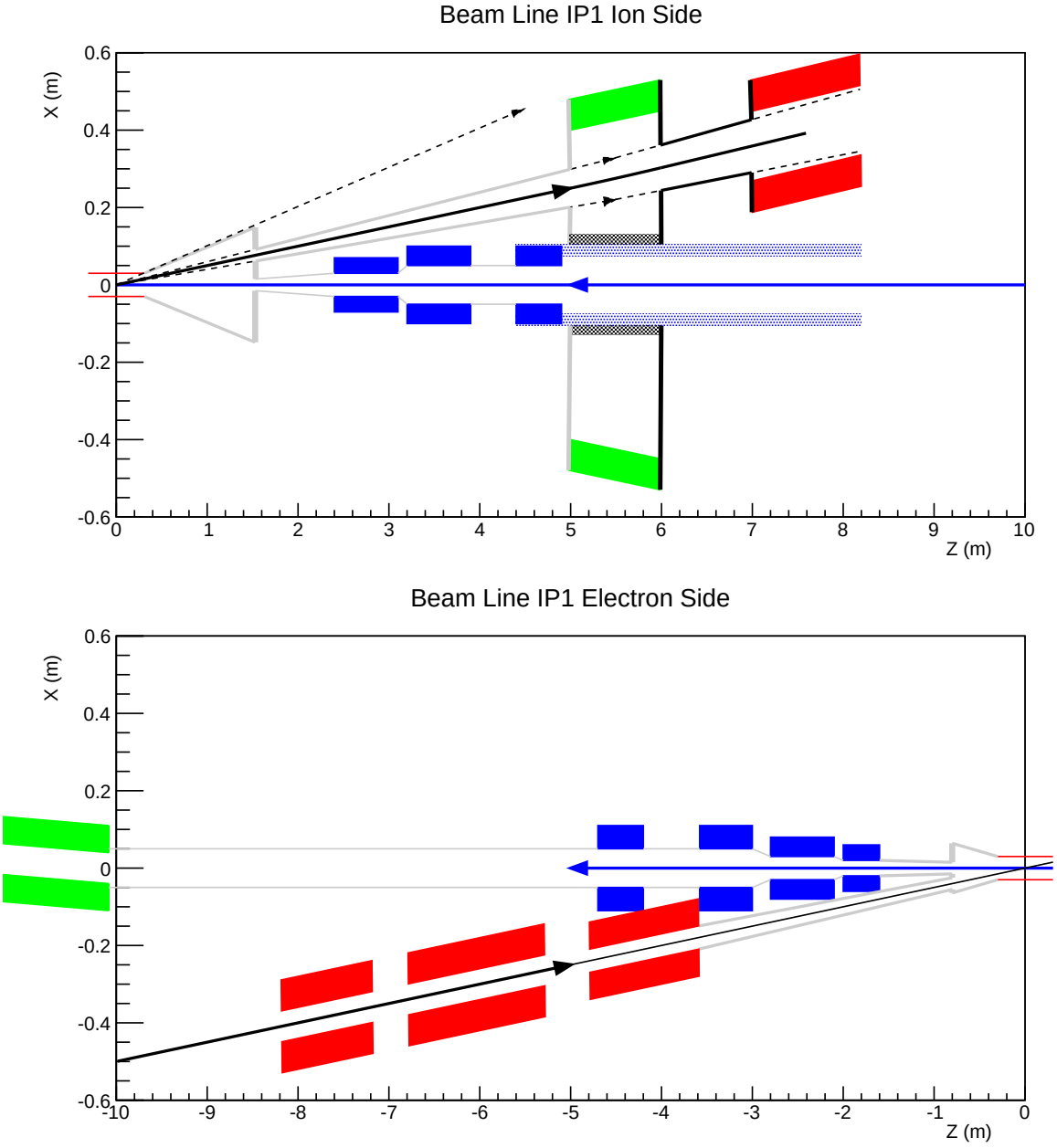

FIG. 1. Initial Beam Pipe design in the central region. **Top:** Ion downstream side; **Bottom:** Ion upstream side. The acceptance of the ion dipole is ±80 mrad. The opening angle of the central flare is 80 mrad in both direction.

A beam pipe configuration in the central region is illustrated in Fig. 1. An alternate design is shown in Fig. 2. In the latter figures, the Ion Dipole acceptance is increased to ±100 mrad. Also, the beam pipe is a straight cone through the dipole, with horizontal opening expanded to accommodate the 6 mrad outward bend of the Dipole.

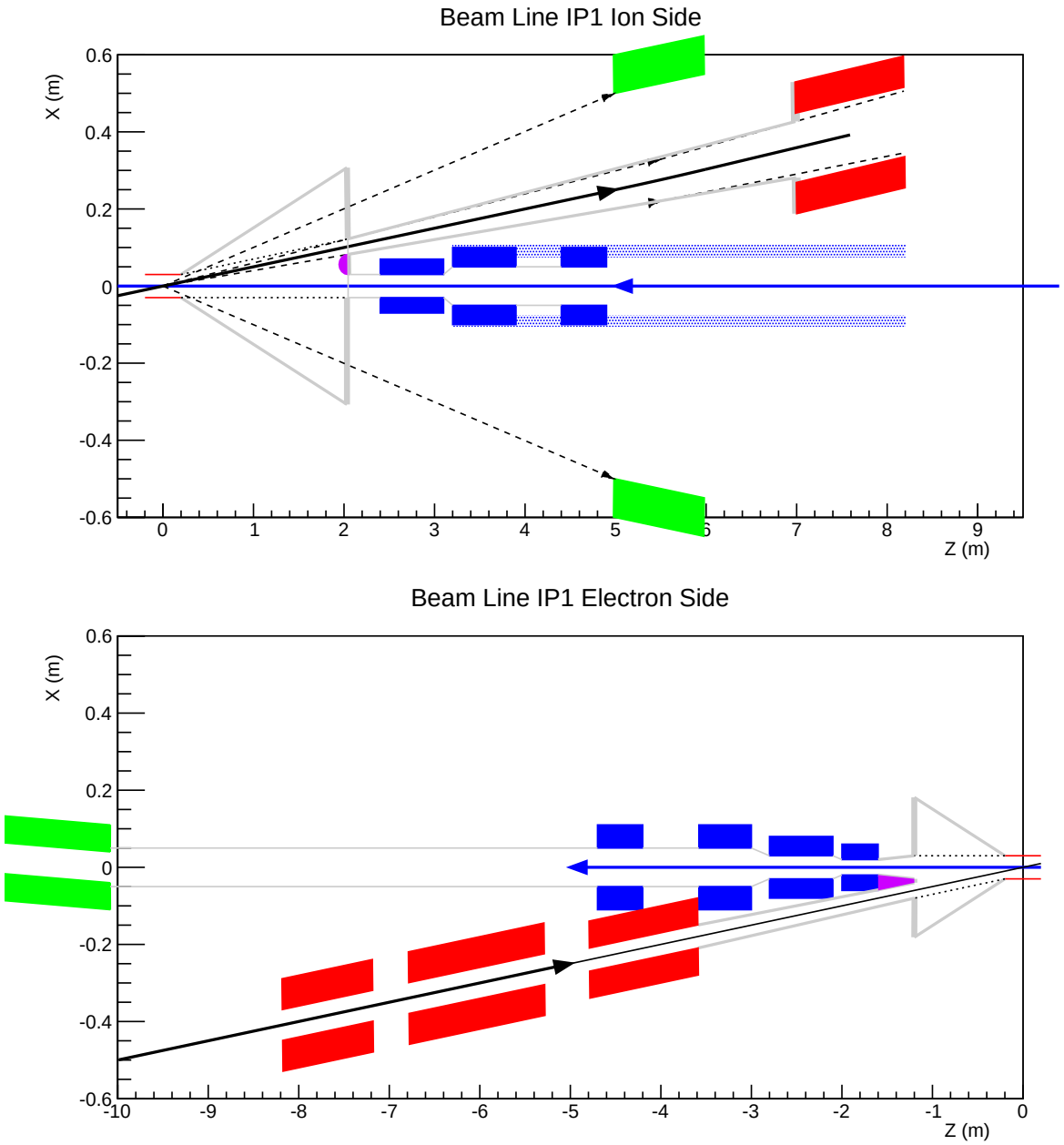

FIG. 2. Improved Beam Pipe design in the central region. **Top** (ion downstream side): The acceptance of the ion dipole is ±100 mrad. A thin mesh for RF impedance matching is included (dotted lines), as well as an RF absorber (violet hemisphere). The angle of the flare is 150 mrad from the electron beam line, and the length of the Be beam pipe (red) is shortened to ±20 cm. This ensures a minimum of 2cm clearance between the ion beam and the wall, even when the IP is shifted ±7.5 cm for synchronization. The end face of the flared beam pipe is a section of a sphere of radius 2.046 m, centered at the nominal IP. **Bottom** (ion upstream, electron downstream side): The acceptance of the flared pipe is ±150 mrad. RF shield mesh (dotted lines) and RF absorber (violet wedge) are also shown. The radius of the spherical end face of the flared section is 1.200 m

A. Vertex Chamber and Initial Beam Pipes

I assume a 1 mm thick Be vertex vacuum chamber of radius 3 cm (or ellipse 3 cm in x and 2 cm in y). I also assume that the minimum radius of the individual electron and ion beam pipes mating to the central chamber is 3.0 cm and 2.0 cm, respectively. The mating distance for the downstream ion beam pipe is therefore:

$$z_1 = \frac{2.0 \text{ cm}}{\tan\theta_{\rm FFQ}} = 2.0455 \text{ meter}. \tag{9}$$

Note that horizontal FFQ acceptance $\theta_{x,\rm FFQ} = 9.78$ mrad (with peak FFQ1 and FFQ2 fields of 8 Tesla). On the other hand, since the vertical FFQ acceptance is $\theta_{y,\rm FFQ} = 12.44$ mrad, at this position, the separate ion beam pipe cross section should be a vertical ellipse of semi-major axes 2.55 cm (vertical) and 2.0 cm (horizontal).

With the straight pipe through the ion Dipole, the axis of the pipe must be offset by 0.9 mrad, to compensate for the 6 mrad bend in the dipole. Thus the beam pipe axis is at 50.9 mrad from the solenoid axis, with an angular opening of ±10.7 mrad Horizontal and 12.44 mrad Vertical. The straight line central length of this conical elliptical pipe is 4.954 m.

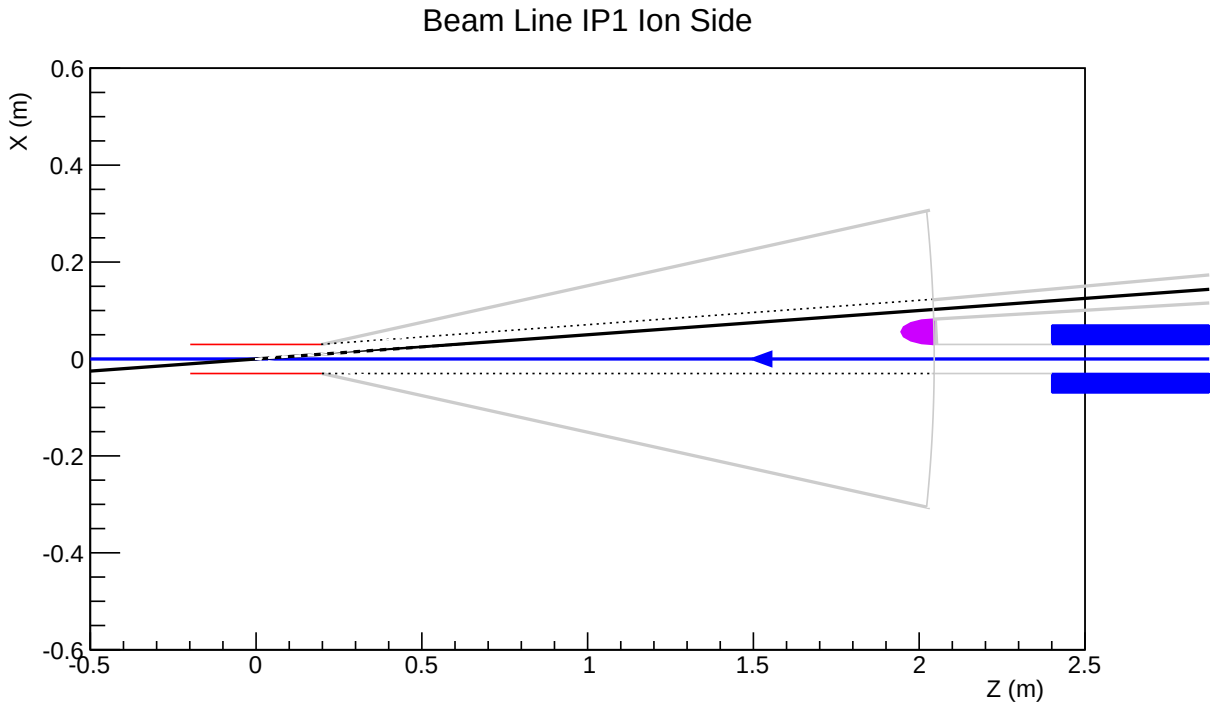

FIG. 3. Detailed view of ion side beam pipe flare at IP, with RF mesh screen (*e.g.* RADIOSCREEN$^{\rm TM}$, Table III) and RF absorber (violet). The RF mesh has a circular cross section at the Be pipe end, but a squashed racetrack shape where it mates to the separate ion and electron beam pipes (Fig. 4). The thickness of the mesh is 0.09 mm, with $X/X_0 = 2 \cdot 10^{-4}$

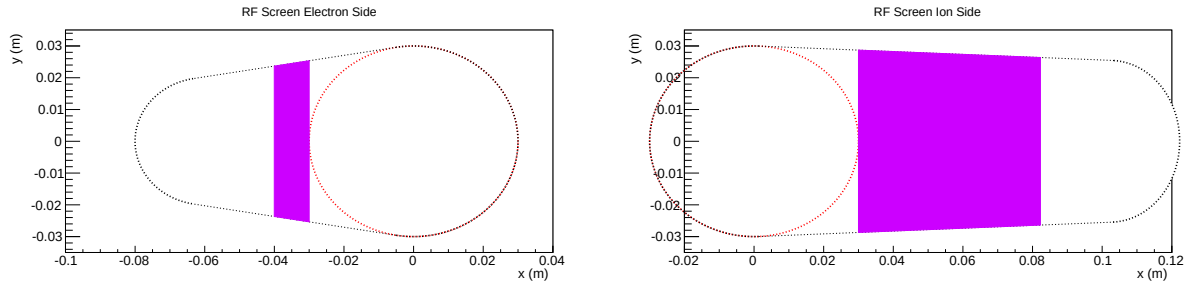

FIG. 4. Cross sections of the RF mesh screens (*e.g.* RADIOSCREEN^{TM}, Table III) and RF absorbers (violet). **Left:** Electron downstream side. The red dotted circle is the profile at $z = -0.2$ m at the matching to the central Be beam pipe. The black dotted race-track is the profile at $z = -1.20$ m where the flare mates to a 3 cm radius electron pipe and a 2 cm radius ion pipe. **Right:** Ion downstream side. The red dotted circle is the profile at $z = +0.20$ m at the the central Be beam pipe. The black dotted race-track outline is the profile at $z = 2.045$ where the flare mates to the elliptical ion pipe and the 3 cm radius electron beam pipe. In both figures, the RF absorber is downstream (electron, ion, respectively) of the screen.

B. RF Shielding Mesh and Absorbers

In the Appendix, I give a very rough estimate of the RF power reflected off an abrupt step in either the electron or ion beam pipe. These estimates are so severe, that even slightly tapering the faces of the flares of Fig. 2 is probably not adequate. Instead, I suggest using a thin RF screen, as depicted in detail in Figs. 3 and 4. With the parameters of Table III, the screen has a thickness of 0.09 mm, or $X/X_0 = 2.0 \cdot 10^{-4}$. Thus even at the shallowest angle of 10 mrad that a detectable particle crosses the mesh, the effective number of radiation lengths is $\leq 2\%$, which is much less than the beam pipe.

At the apex of the junctions between the electron and ion vacuum pipes, it is impossible to avoid a step in the wave impedance. This can perhaps be compensated by placing in the vacuum RF absorber material, as indicated in violet in Figs. 2, 3, 4.

C. Final Focus Quadrupoles

The beam pipe through the ion downstream FFQ triplet should be at the full diameter of the quadrupole apertures, since particles will be successively focussed and defocused. The quadrupoles themselves will be the beam pipe, with flanges at each end for attaching the joining sections. The specifications for the beam pipe in the drift spaces are:

- Between Q1 and Q2: 1 meter gap, 10 cm radius at exit of Q1, expanding to 17.6 cm radius at entrance to Q2 (Half angle of cone = 76 mrad).
  Conical Al pipe, wall thickness $t = (3.45\%)(17.6 \text{ cm}) = 0.60$ cm.

- Between Q2 and Q3: Conical Al pipe 1 meter long, 17.6 cm radius at exit of Q2, 19.4

cm at entrance to Q3 (Cone half-angle = 18 mrad).
Wall thickness $t = (3.45\%)(19.4\text{ cm}) = 0.67$ cm.

D. Entrance to Downstream Ion Final Focus Q1

The acceptance of FFQ triplet is elliptical, with semi-major vertical axis 14 mrad and semi-minor horizonatal axis 11 mrad (for 9 Tesla fields, or 9.78 and 12.44 at 8 Tesla). It will therefore maximize the tracking acceptance of the Forward region if the beam pipe upstream of Q1 is an elliptical cone, tapering at approximately 12.44 mrad in the vertical and 9.78 mrad in the horizontal (see below) with geometrical size at the entrance to Q1 of (7 m)(14 mrad) = 10 cm vertical, and (7 m)(11 mrad) = 7.7 cm horizontal.

TABLE IV. Summary of Beam Pipe Design. All Z-coordinates are absolute, with $-Z$ along the electron beam direction and $Z = 0$ at solenoid center. Nominal IP position is $Z_{\rm IP} = -0.5$ m. This convention disagrees with the rest of this note, in which $z = 0$ at the IP.

Beam Elements	Material	Shape	Radius (cm)	Thickness (mm)	(Z_1, Z_2) (m)
Ion Side					
Vertex Chamber	Be	Straight-Circular	3	1	$(-0.698, -0.298)$
Flare	Al/CFC	Conical: ± 150 mrad	3 to 30.9 Z_1 to Z_2	1 to 10 taper	$(-0.30, 1.522)$
Spherical Face	Al/CFC	Spherical center at $Z_{\rm IP}$	204.5	≤ 10	$(1.522, 1.545)$
Electron Pipe to eFFQ1	Al	Straight-Circular	3	1	$(1.545, 2.250)$
Ion Pipe to iFFQ1	Al/CFC	Elliptical Conical Opening Angles, radii (x, y) $(\pm 10.7, \pm 12.44)$ mrad	Axis 50.9 mrad to Z-axis $(2.0, 2.55)$ $(7.3, 8.7)$	1 3	at $Z_1 = 1.543$ m at $Z_2 = 6.491$ m
Electron Side					
Flare	Al/CFC	Conical: 150 mrad ± 150 mrad	3 to 17.9 Z_1 to Z_2	1 to 5 taper	$(-0.698, -1.687)$
Spherical Face	Al/CFC	Spherical center at $Z_{\rm IP}$	120.0	≤ 10	$(-1.687, -1.700)$
Electron Pipe to eFFQ1	Al	Conical-Circular	3 to 2	1	$(-1.700, -2.100)$
Ion Pipe to iFFQ1	Al	Conical-Circular	2 to 3	1	$(-1.698, -4.090)$

Appendix A: Reflections at a Boundary

I consider the Liénard-Wiechert fields of a relativistic moving charge to make a naïve estimate of the effect of an abrupt transition of the radius of a beam pipe. For a point

charge Ne moving at constant velocity $\beta c\hat{z}$, the total electromagnetic energy in cylindrical annulus of inner and outer radii ρ_1 and ρ_2 is (Gaussian units):

$$\mathcal{E} = 2\pi \int_{\rho_1}^{\rho_2} \int_{-\infty}^{\infty} dz \frac{1}{8\pi} \left[\mathbf{E}^2 + \mathbf{B}^2\right] \approx (Ne)^2 \frac{\pi}{8} \left[\frac{1}{\rho_1} - \frac{1}{\rho_2}\right] \gamma \tag{A1}$$

If the bunch frequency is f, then as the beam pipe makes a sudden transition from radius ρ_2 to ρ_1, we can estimate the reflected power as:

$$\mathcal{P} = \mathcal{E} f \tag{A2}$$

With $f = 0.476$ GHz and $0.66 \cdot 10^{10}$ protons per bunch at 100 GeV/c ($\gamma \approx 100$), if the pipe makes an abrupt transition from 6 cm radius to 3 cm radius, the reflected power is approximately 3.3 kWatt.

To avoid this reflection and disruption, the beam pipe transitions either need to be smooth, or hidden behind a mesh, or must include RF absorbers. All three options are implemented in the design outlined here.

---

[1] S. Abeyratne, D. Barber, A. Bogacz, P. Brindza, Y. Cai, A. Camsonne, A. Castilla and P. Chevtsov *et al.*, "MEIC Design Summary," arXiv:1504.07961 [physics.acc-ph].

[2] V. Morozov, Workshop on *High Energy Nuclear Physics with Spectator Tagging,* , 9–11 March 2015, Old Dominion University, `http://www.jlab.org/indico/event/Tagging2015`

[3] C. Hauviller, "Design rules for vacuum chambers," `https://cds.cern.ch/record/1046848/files/p31.pdf`,

[4] K. A. Olive *et al.* [Particle Data Group Collaboration], "Review of Particle Physics," Chin. Phys. C **38**, 090001 (2014). `http:pdg.lbl.gov`

[5] F. Lin, MEIC Detector Integration Meeting, 10 June 2015 `https://eic.jlab.org/internal/index.php/Detector_Working_Group_Meetings`